

1 **Catalytic Conversion of Bamboo Sawdust Over ZrO₂-CeO₂/γ-Al₂O₃**
2 **to Produce Ketonic Hydrocarbon Precursors and Furans**

3 Jia Wang ^{*,†,‡}, Chao Xu ^{*,†}, Zhaoping Zhong ^{*,†}, Aidong Deng [§], Najia Hao [‡], Mi Li [‡],
4 Xianzhi Meng [‡], Arthur J. Ragauskas ^{*,‡,#,⊥}

5 [†]*Key Laboratory of Energy Thermal Conversion and Control of Ministry of Education,*
6 *Southeast University, No.2 Sipailou, Xuanwu District, Nanjing, Jiangsu 210096, China*

7 [‡]*Department of Chemical & Biomolecular Engineering, University of Tennessee,*
8 *Knoxville, Tennessee 37996, USA*

9 [§]*National Engineering Research Center of Turbo-generator Vibratio, Southeast*
10 *University, No.2 Sipailou, Xuanwu District, Nanjing 210096, Jiangsu Province, China*

11 [#]*Department of Forestry, Wildlife and Fisheries, Center for Renewable Carbon, the*
12 *University of Tennessee, Institute of Agriculture, Knoxville, TN 37996, USA*

13 [⊥]*Joint Institute for Biological Science, Biosciences Division, Oak Ridge National*
14 *Laboratory, Oak Ridge, TN 37831, USA*

15
16 **Abstract**

17 A series of metal oxides including ZrO₂/γ-Al₂O₃, CeO₂/γ-Al₂O₃, and ZrO₂-CeO₂/γ-
18 Al₂O₃ were synthesized and employed to conduct catalytic fast pyrolysis of bamboo
19 sawdust via an analytical pyrolyzer-gas chromatograph/mass spectrometer (Py-GC/MS)
20 to produce hydrocarbon precursors such as ketones and furans. Experimental results
21 illustrated that the use of metal oxides enhanced the formation of ketones and
22 monoaromatic hydrocarbons compared to catalyst-free trial. Among the metal oxides,
23 ZrO₂-CeO₂/γ-Al₂O₃ exhibited the most significant ketonization and aldol condensation

24 activities yielding the highest concentration of linear and cyclic ketones. In addition,
25 non-acidic oxygenates such as furfural, acetol, butanedial, 2,3-dihydrobenzofuran and
26 methyl acetate, were efficiently converted into hydrocarbon precursors over metal
27 oxides. A dual catalytic bed system integrating $ZrO_2-CeO_2/\gamma-Al_2O_3$ and HZSM-5
28 significantly facilitated the production of aromatic hydrocarbons compared to pure
29 HZSM-5 catalytic run. The use of $ZrO_2-CeO_2/\gamma-Al_2O_3$ mixed with HZSM-5 mode
30 maximized the formation of xylenes, while $ZrO_2-CeO_2/\gamma-Al_2O_3$ mixed with bamboo
31 sawdust catalytic trial increased the concentration of benzene, toluene, and
32 alkylbenzenes.

33 **Key words**

34 Metal oxide catalysts; $ZrO_2-CeO_2/\gamma-Al_2O_3$; Hydrocarbon precursors; Dual catalytic bed
35 system; Aromatic hydrocarbons.

36 **Introduction**

37 The continued consumption of limited fossil fuel reserves at an increasing rate along
38 with environmental concerns has motivated many researchers to develop renewable
39 alternatives. Lignocellulosic biomass is a carbon-neutral energy source that is widely
40 available for the production of liquid fuels (i.e., biofuels) and other value-added
41 chemicals¹⁻³. Fast pyrolysis of biomass is an active field of research directed at yielding
42 a viable biofuel resource. It is now well known that this bio-oil is a complex mixture of
43 oxygenates which needs chemical upgrading to minimize oxygen functionality as these
44 groups detrimentally impact fuel properties such as corrosivity, ignition point,
45 hydrocarbon solubility and other fuel properties⁴⁻⁶. Although hydro-treatments can
46 deoxygenate pyrolysis oils, the costs associated with this process are prohibitively high
47 hence research studies have shifted to alternative catalytic deoxygenation routes to yield
48 upgraded hydrocarbon fuel alternatives⁷⁻⁹.

49 Among the strategies used to upgrade pyrolysis oils, direct catalytic upgrading over
50 metal oxides and/or acidic zeolites to produce renewable drop-in hydrocarbon

51 precursors provides a promising thermochemical approach as it could relieve the
52 intensive hydrogenation conditions during hydrodeoxygenation (HDO) process
53 compared to non-catalytic bio-oil ¹⁰. In particular, converting pyrolytic primary
54 oxygenates into monofunctional rich intermediates such as alkylphenols, furans and
55 ketones, has received considerable attention ^{7, 11-15}. Mullen et al. ⁷ studied the role of
56 potassium exchange in catalytic pyrolysis of biomass over ZSM-5, and experimental
57 results indicated that the use of modified K/ZSM-5 provided a ~3-4-fold increase in the
58 yields of alkylphenols and 2-methylfuran compared to noncatalytic and HZSM-5
59 catalyzed runs. Bohre et al. ¹³ investigated the upgrading of 5-hydroxymethylfurfural
60 to C9 and C11 fuels over $Zr(CO_3)_x$, and they found that the product mixture contained
61 almost 92% C9–aldol products.

62 Concerning the formation of ketones during catalytic fast pyrolysis of biomass, it is
63 well known that ketonization and aldol condensation reactions over metal oxides are
64 attractive as a means of promoting C-C coupling reactions with the removal of oxygen
65 via dehydration ¹⁶⁻¹⁷. A number of metal oxides, such as TiO_2 , ZrO_2 , and CeO_2 , have
66 been examined extensively in the HDO process to convert acids into ketones ¹⁷⁻²². In
67 contrast, direct conversion of other primary pyrolytic oxygenates such as aldehydes and
68 esters into ketones has received far less attention, in particular for a one-step catalytic
69 upgrading process at ambient pressure in the absence of external H_2 . Additionally, the
70 total yield of carboxylic acids obtained in the pyrolysis of lignocellulosic biomass is
71 ~3-6 wt% ²³, hence converting other non-acidic primary oxygenates into ketones is
72 essential to achieve ketone rich hydrocarbon precursors. In this case, Mante et al. ⁸
73 conducted catalytic fast pyrolysis of sugar maple over a series of metal oxides via an
74 analytical Py-GC/MS, and it was found that cerium-based oxides were effective in the
75 conversion of primary pyrolytic vapors into ketones. They also observed that non-acidic
76 oxygenates such as hydroxyacetaldehyde could be transformed into ketones over pure
77 CeO_2 . However, the effect of metal oxides on the formation of furans, and subsequent
78 conversion of ketonic intermediates into aromatic hydrocarbons over acidic zeolites by
79 a one-step process have not been examined. Furthermore, pure CeO_2 has a relatively
80 small surface area (~81 m^2/g for meso- CeO_2) which might hinder the ketonization and

81 aldol condensation reactions regarding catalytic upgrading of lignocellulosic biomass
82 ²⁴⁻²⁵, and this effect could be minimized using a catalyst support.

83 In this study, a number of metal oxides, including $\text{ZrO}_2/\gamma\text{-Al}_2\text{O}_3$, $\text{CeO}_2/\gamma\text{-Al}_2\text{O}_3$ and
84 $\text{ZrO}_2\text{-CeO}_2/\gamma\text{-Al}_2\text{O}_3$ were synthesized and characterized, and then were initially used to
85 conduct catalytic fast pyrolysis of bamboo sawdust via an analytical Py-GC/MS to
86 produce ketonic rich hydrocarbon intermediates. In addition, conversion of furfural into
87 furans and transformation of other non-acidic oxygenates into ketones were also studied.
88 Finally, a dual catalytic bed system was examined using $\text{ZrO}_2\text{-CeO}_2/\gamma\text{-Al}_2\text{O}_3$ and
89 HZSM-5 to further convert hydrocarbon precursors into aromatic hydrocarbons by a
90 one-step process.

91 **Experimental**

92 **Materials**

93 Bamboo sawdust was obtained from Huzhou, Zhejiang province, China. The samples
94 were ground and sieved with a 100 screen mesh (~ 0.15 mm), and then were dried at
95 105°C for 24 h prior to conducting catalytic fast pyrolysis experiments. The ultimate
96 analysis of bamboo sawdust was conducted by Vario EL II elemental analyzer
97 (Germany), and the results were shown in Table 1.

98 **Table 1. Ultimate analysis of bamboo sawdust**

Ultimate analysis ^a (%)	C	H	O ^b	N	S
Bamboo sawdust	51.5	6.1	42.1	0.2	0.1

99 ^a dry-ash free basis; ^b by difference;

100 HZSM-5 zeolites ($\text{SiO}_2/\text{Al}_2\text{O}_3=46$) were provided by the Catalyst Plant of Nankai
101 University, Tianjin, China. The physicochemical properties are shown in Table S1. All
102 the chemicals used in the synthesis of metal oxide catalysts including $\text{Al}(\text{NO}_3)_3\cdot 9\text{H}_2\text{O}$,
103 $\text{ZrO}(\text{NO}_3)_2\cdot 5\text{H}_2\text{O}$ and $\text{Ce}(\text{NO}_3)_3\cdot 6\text{H}_2\text{O}$, were supplied by Nanjing Chemical Reagent
104 Co. Ltd.

105 **Catalyst preparation**

106 The metal oxide catalysts were prepared according to a literature precipitation
107 method ²⁶. For a typical run, 29.4 g Al(NO₃)₃·9H₂O and 3.5 g ZrO(NO₃)₂·5H₂O were
108 dissolved in deionized water under vigorous stirring conditions and ultrasonicated at 35
109 °C for 45 min. A NH₄HCO₃ solution (10.0 wt%) was used to adjust the pH of aqueous
110 solution (~8.5), and the resulting white precipitate was filtered and washed with DI
111 water. Finally, the obtained samples were dried at 110 °C for 10 h, and then were
112 calcined at 500 °C for 4 h in a muffle furnace. The finished catalyst ZrO₂/γ-Al₂O₃ was
113 labeled as ZrO₂/A with 20 wt% ZrO₂. In addition, γ-Al₂O₃, CeO₂/γ-Al₂O₃ and ZrO₂-
114 CeO₂/γ-Al₂O₃ with 8 wt% CeO₂ (using Ce(NO₃)₃·6H₂O) were produced by the same
115 procedure as described above. CeO₂/γ-Al₂O₃ and ZrO₂-CeO₂/γ-Al₂O₃ were labeled as
116 CeO₂/A and ZrO₂-CeO₂/A, respectively.

117 **Catalyst characterization**

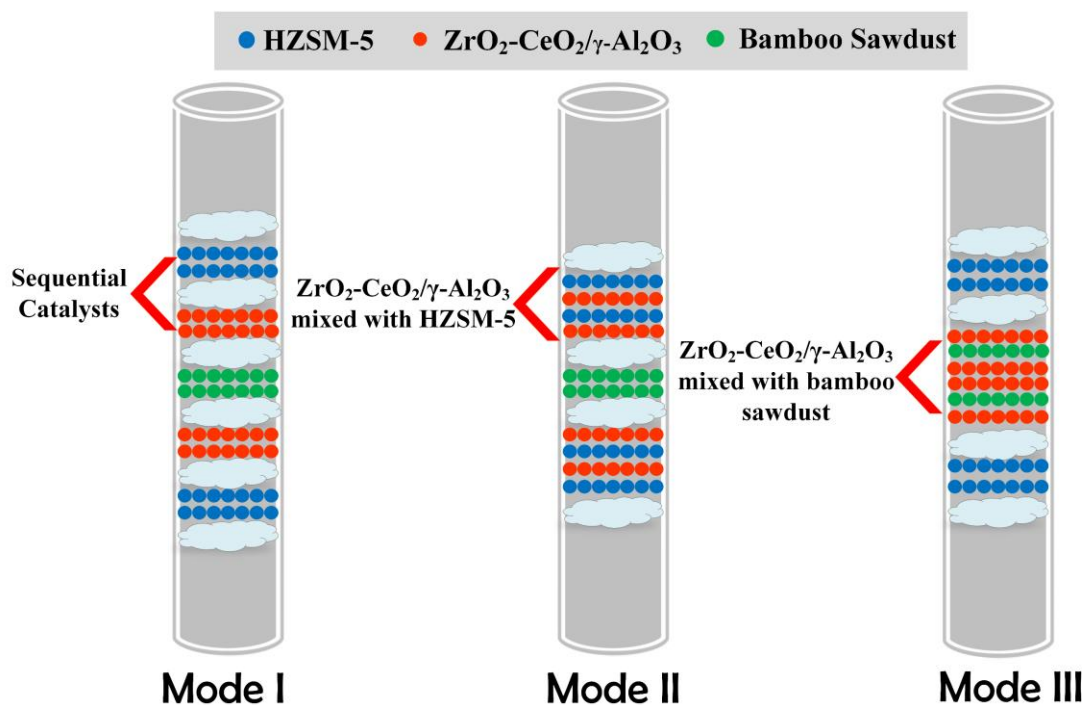
118 The powder X-ray diffraction (XRD) patterns were conducted by Bruker D8 Focus
119 using CuKα radiation with a step of 0.02 at a current of 40mA and a voltage of 40 kV.
120 The scanning range of 2θ was from 5° to 90° with a 10 min⁻¹ scanning rate. To measure
121 the surface properties and pore characteristics of synthesized metal oxide catalysts,
122 nitrogen adsorption–desorption isotherms were conducted by a ASAP2400
123 (Micromeritics, USA) adsorption instrument with N₂ at 77K. The surface area of
124 synthesized metal oxide was calculated by BET method, and the pore size and pore
125 volume were calculated using the BJH method ²⁶.

126 **Experimental methods**

127 A CDS analytical Pyroprobe 5200 pyrolyzer was used to conduct catalytic fast
128 pyrolysis of bamboo sawdust, and the pyrolytic chemicals were identified in a
129 connected gas chromatography/mass spectrometry (GC/MS, 7890A/5975C, Agilent).
130 For a typical run, 1 mg (± 0.01 mg) powdered bamboo sawdust was loaded into an
131 open-ended quartz tube (20 mm in length and 2 mm in diameter), and catalyst to

132 biomass mass ratio was kept at 2:1 to ensure enough retention time of pyrolytic vapors
133 in the catalyst bed. Moreover, two catalyst beds around biomass feedstocks were used
134 because pyrolysis vapors leave from both sides of the quartz tube and both catalyst beds
135 participated in catalytic reactions of pyrolysis vapors²⁷. The pyrolyzer was heated at 20
136 °C/ms to 600 °C and then was held for 20 s. High pure analytical helium (99.999%) was
137 used as inert gas for pyrolysis and carrier gas for GC/MS. Detailed information and
138 reaction conditions of Py-GC/MS could be found in Figure S1 and elsewhere²⁸⁻²⁹. The
139 identification of pyrolytic compounds was conducted by comparing mass spectra with
140 the NIST MS library database, and total ion chromatogram (TIC) area of chromatogram
141 peaks was used to analyze the relative concentration of identified products, which is the
142 same methodology as recently reported by Lu et al.³⁰ and Sebestyén et al.³¹.

143 HZSM-5 zeolites and $\text{ZrO}_2\text{-CeO}_2/\gamma\text{-Al}_2\text{O}_3$ were used to form a dual catalytic bed
144 system. Three different catalytic modes were explored as shown in Figure 1.
145 Specifically, Mode I was a sequential catalytic run, HZSM-5 and $\text{ZrO}_2\text{-CeO}_2/\gamma\text{-Al}_2\text{O}_3$
146 were separately placed in the quartz tube, and pyrolytic vapors were first catalyzed by
147 $\text{ZrO}_2\text{-CeO}_2/\gamma\text{-Al}_2\text{O}_3$ to produce hydrocarbon precursors, and then the obtained
148 intermediates were sequentially aromatized by HZSM-5. Concerning Mode II, HZSM-
149 5 and $\text{ZrO}_2\text{-CeO}_2/\gamma\text{-Al}_2\text{O}_3$ were mixed thoroughly before each experiment, and
150 pyrolytic volatile matters were simultaneously catalyzed by the catalyst blends. Finally,
151 for Mode III, $\text{ZrO}_2\text{-CeO}_2/\gamma\text{-Al}_2\text{O}_3$ was mixed with bamboo sawdust to form an in-situ
152 catalytic trial, and then the obtained pyrolytic products were subsequently catalyzed by
153 HZSM-5. Note that in order to completely convert ketones and furans into aromatic
154 hydrocarbons, catalyst to biomass ratio was increased to 4:1 when the dual catalytic
155 bed system was used to conduct pyrolysis of bamboo sawdust, and HZSM-5 to $\text{ZrO}_2\text{-}$
156 $\text{CeO}_2/\gamma\text{-Al}_2\text{O}_3$ mass ratio was kept at 4:1. Each experiment was conducted at least twice
157 to confirm reproducibility.



158

159 **Figure 1.** Dual catalytic bed system used in catalytic fast pyrolysis of bamboo sawdust.

160 **Results and discussion**

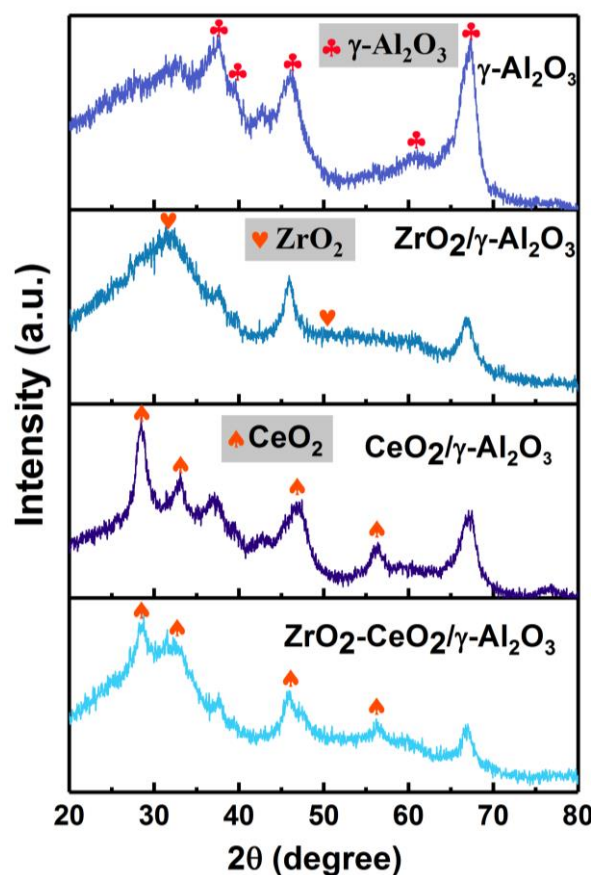
161 **Structural and morphological properties of synthesized metal oxides**

162 The textural properties of synthesized catalysts regarding surface area, pore volume
 163 and size are summarized in Table 2 (acidic properties were shown in Figure S2). All
 164 specimens presented a type IV isotherm with H2-type hysteresis (shown in Figure S3),
 165 which indicated that a typical mesoporous structure was obtained for the prepared
 166 catalysts ²⁶. As shown in Table 2, γ-Al₂O₃ has a large surface area (228 m²/g) and a
 167 well-developed pore volume (0.68 cm³/g). However, the surface area decreased to 173
 168 m²/g for ZrO₂/γ-Al₂O₃, 160 m²/g for CeO₂/γ-Al₂O₃, and 162 m²/g for ZrO₂-CeO₂/γ-
 169 Al₂O₃, which might be attributed to the filling of pores with ceria or zirconia particles
 170 ³². Similarly, pore volume presented the same trend, which was consistent with other
 171 works ^{26,32}. In addition, all the samples exhibited mesoporous properties with a ~10 nm
 172 pore diameter, hence it might be beneficial to the diffusion of pyrolytic vapors during
 173 catalytic upgrading process.

174 **Table 2. Physical properties of synthesized metal oxides.**

Catalysts	BET surface area (m ² /g)	Pore volume (cm ³ /g)	Pore adsorption diameter (nm)	Pore desorption diameter (nm)
γ -Al ₂ O ₃	228	0.68	14.0	11.8
ZrO ₂ / γ -Al ₂ O ₃	173	0.55	10.1	9.5
CeO ₂ / γ -Al ₂ O ₃	160	0.53	13.2	10.7
ZrO ₂ -CeO ₂ / γ -Al ₂ O ₃	162	0.54	12.1	11.3

175 Figure 2 shows the XRD results of γ -Al₂O₃, ZrO₂/ γ -Al₂O₃, CeO₂/ γ -Al₂O₃ and ZrO₂-
 176 CeO₂/ γ -Al₂O₃. As anticipated, all diffraction peaks attributed to γ -Al₂O₃ ($2\theta=36.6^\circ$,
 177 39.7° , 46.1° , 60.8° and 66.6°) were detected, and the peak intensity was weakened after
 178 doping with CeO₂ ($2\theta=28.6^\circ$, 33.2° , 47.6° and 56.4°) or ZrO₂ ($2\theta=30.4^\circ$ and 50.5°). For
 179 the ZrO₂-CeO₂/ γ -Al₂O₃ metal oxide, peaks corresponding to ZrO₂ were negligible due
 180 to Zr₄⁺ ions which could incorporate into CeO₂ crystal lattice to form a homogeneous
 181 solid solution ²⁶.



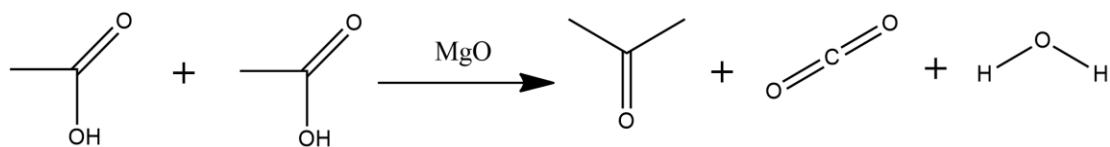
182

183 **Figure 2.** X-ray diffraction (XRD) patterns of synthesized metal oxides.

184 **Catalytic fast pyrolysis of bamboo sawdust over synthesized metal oxides**

185 Generally, organic products derived from pyrolysis of lignocellulosic biomass can be
186 classified into acids, phenols, ketones, furans, esters and aldehydes, and in this work,
187 we focused on the formation of ketonic products from acids and other non-acidic
188 oxygenates. Figure 3 presents the pyrolytic products originated from catalytic fast
189 pyrolysis of bamboo sawdust over various metal oxides (detailed products shown in
190 Table S2-S5). As shown in Figure 3a, all the metal oxides enhanced the production of
191 ketones compared to non-catalytic pyrolysis run, and the highest concentration of
192 ketones was achieved over ZrO_2 - CeO_2/γ - Al_2O_3 and followed by CeO_2/γ - Al_2O_3 . It was
193 reported that ketonization reaction was responsible, for instance, acetic acid, a typical
194 compound obtained from thermal conversion of biomass, can readily undergo
195 ketonization process in the presence of a base catalyst as shown in Scheme 1 ³³.

196



198

Scheme 1. Ketonization pathway of acetic acid over MgO.

199 Typically, bulk and surface catalytic ketonization are two pathways for converting
200 acetic acid into ketones, depending on the metal oxides employed ³⁴. For metal oxides
201 with low basicity or high lattice energies such as CeO_2 , ZrO_2 , and TiO_2 , pyrolytic vapors
202 are catalyzed on the surface of catalyst. On the other hand, metal oxides with high
203 basicity or low lattice energies including MgO and CaO (shown in our previous works
204 ^{28, 35}), interact strongly with acetic acid to form a metal carboxylate via bulk
205 ketonization. Furthermore, Snell and co-authors ³⁶ concluded that CeO_2 promoted
206 ketonization by the production of a metal carboxylate intermediate through either the
207 surface or bulk pathway. Therefore, catalytic fast pyrolysis bamboo sawdust over
208 CeO_2/γ - Al_2O_3 produced more ketones than that over ZrO_2/γ - Al_2O_3 , along with a lower
209 concentration of acids as shown in Figure 3b.

210 In addition, among the metal oxide catalysts used in present work, ZrO₂-CeO₂/γ-
211 Al₂O₃ illustrated the most prominent ketonization performance and this was attributed
212 to high oxygen content and exchangeability, strong Lewis basicity, enhanced vacancy
213 sites and redox performances of CeO₂^{26,37}. Furthermore, an addition of ZrO₂ to CeO₂
214 resulted in the production of a highly defective surface, which further enhanced the
215 ketonization activity²⁶.

216 Phenol and alkylphenols are important materials for the production of plastics,
217 pharmaceuticals, and other fine chemicals⁷. As shown in Figure 3c and 3d, compared
218 to non-catalytic pyrolysis trial, all the metal oxides increased the generation of phenol
219 and alkylphenols and decreased the formation of alkoxy phenols, which was consistent
220 with previous studies^{8,33}. The highest formation of light phenolic compounds was
221 obtained over CeO₂/γ-Al₂O₃, followed by ZrO₂-CeO₂/γ-Al₂O₃. Concerning aromatic
222 hydrocarbons, as shown in Figure 3e, no aromatic hydrocarbons were identified in the
223 noncatalytic pyrolysis run. However, monoaromatic hydrocarbons including toluene
224 and xylenes were detected when metal oxides were used as catalysts to pyrolyze the
225 bamboo sawdust. The highest relative abundance of monoaromatic hydrocarbons was
226 achieved using ZrO₂-CeO₂/γ-Al₂O₃, which indicated its stronger dehydration activity
227 than ZrO₂/γ-Al₂O₃ and CeO₂/γ-Al₂O₃.

228 In the case of furans, as exhibited in Figure 3f, furfural was a predominant product
229 in the noncatalytic pyrolysis run, and it is an undesired compound due to its contribution
230 to pyrolysis oil thermal instability⁷. It is worth noting that the use of metal oxides
231 completely transformed furfural with the formation of monofunctional furans such as
232 2,5-dihydrofuran, 2-methylfuran, and 2,5-dimethylfuran. CeO₂/γ-Al₂O₃ showed the
233 most robust catalytic activity with the highest concentration of total monofunctional
234 furans.

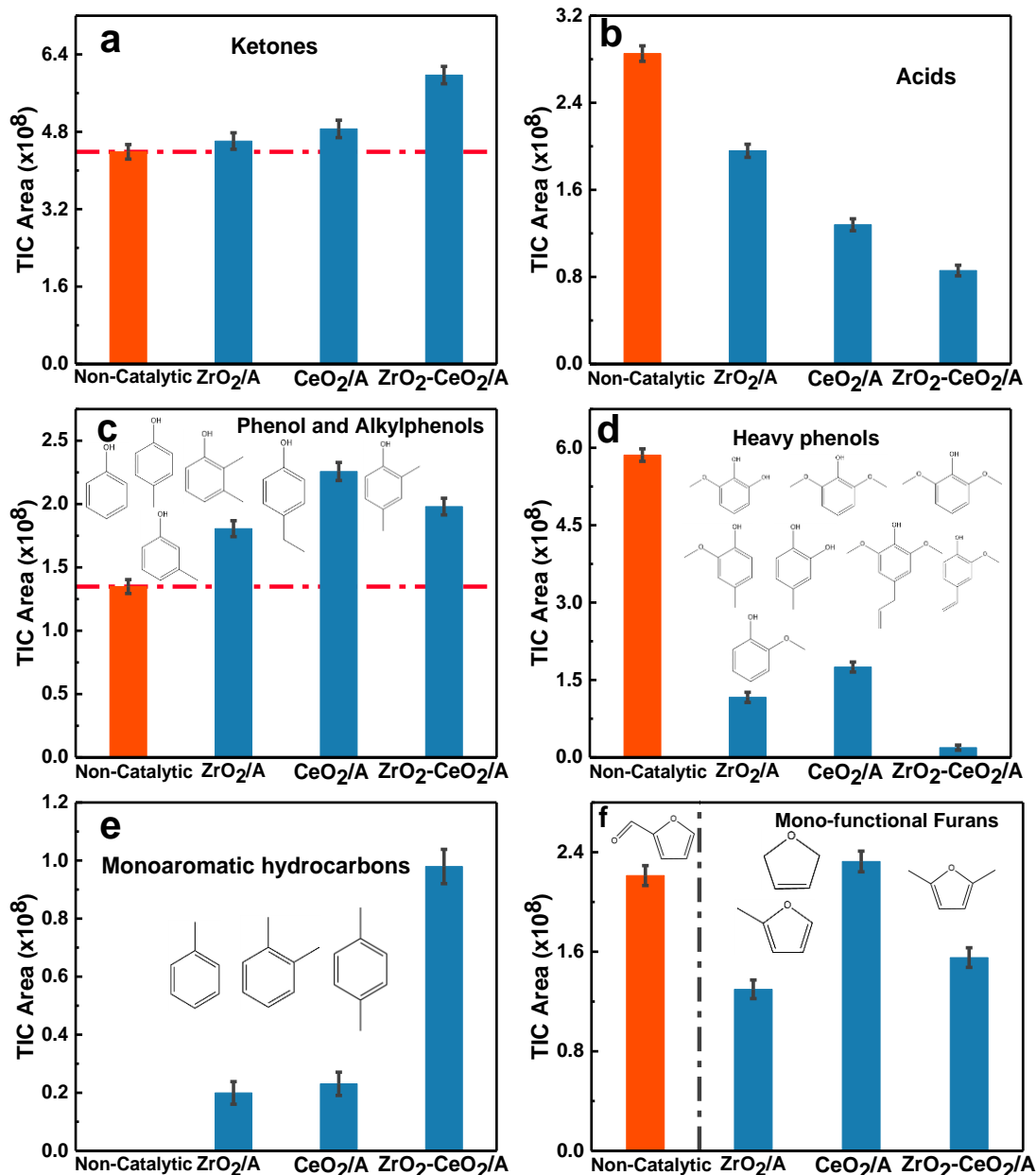


Figure 3. Products obtained from catalytic fast pyrolysis of bamboo sawdust over metal oxides: (a) ketones; (b) acids; (c) phenol and alkylphenols; (d) heavy phenols; (e) monoaromatic hydrocarbons; (f) furans. The inset structures are representative compounds detected in each group.

Distribution of ketones

The ketones identified by GC/MS obtained from catalytic fast pyrolysis of bamboo sawdust over metal oxides could be classified into linear and cyclic ketones, and the dominated linear ketones were acetone, 2-butanone, 2,3-butanedione, 2,3-pentanedione

246 and 2-pentanone. The main cyclic ketones were cyclopentanone and 2-cyclopenten-1-
247 one. As summarized in Figure 4, in comparison to noncatalytic pyrolysis trial, the same
248 reaction over $ZrO_2-CeO_2/\gamma-Al_2O_3$ enhanced the formation of acetone (Figure 4a) and
249 cyclic ketones (Figure 4d and 4e). For instance, the relative selectivity of cyclic ketones
250 was 31.5% for the catalyst-free trial, while it increased to 44.2% on $ZrO_2-CeO_2/\gamma-Al_2O_3$
251 catalyzed run (shown in Figure 5), which exhibited promising cyclization and ketonic
252 decarboxylation properties. Moreover, complete elimination of 3,5-
253 dimethoxyacetophenone was achieved in the presence of $ZrO_2-CeO_2/\gamma-Al_2O_3$. 3,5-
254 dimethoxyacetophenone was the main heavy ketone detected in thermal conversion of
255 bamboo sawdust³⁸⁻³⁹, and the relative selectivity reached to 26.4% (Figure 5). Dong et
256 al.³⁹ studied the effect of various acid washing pretreatments of bamboo on product
257 distributions of pyrolysis oils, and they found that these treatments slightly lowered the
258 concentration of 3,5-dimethoxyacetophenone. Therefore, all the metal oxides studied
259 in present work clearly demonstrate promise for inhibiting the generation of 3,5-
260 dimethoxyacetophenone.

261 Regarding the highly oxygenated diketones such as 2,3-butanedione and 2,3-
262 pentanedione generated under noncatalytic fast pyrolysis (shown in Figure 4b), the use
263 of metal oxides lowered the concentration as the conversion rate was 27.5% for $ZrO_2/\gamma-$
264 Al_2O_3 , 31.3% for $CeO_2/\gamma-Al_2O_3$, and 38.9% for $ZrO_2-CeO_2/\gamma-Al_2O_3$, respectively.
265 Similar results have been found by Mante and co-workers using pure CeO_2 as a catalyst
266 to convert sugar maple into hydrocarbon precursors⁸. They concluded that catalyst to
267 biomass ratio was responsible for the low conversion of diketones, and at a high catalyst
268 to biomass ratio of 15:1, they observed that these oxygenates were transformed to
269 aromatic hydrocarbons without any production of ketones. Therefore, we further
270 conducted comparative studies for increasing the catalyst to biomass ratio to 4:1, 6:1
271 and 8:1 (shown in Table S6-S8), and it was found that there were no diketones formed
272 when the catalyst to biomass ratio was regulated at 4:1.

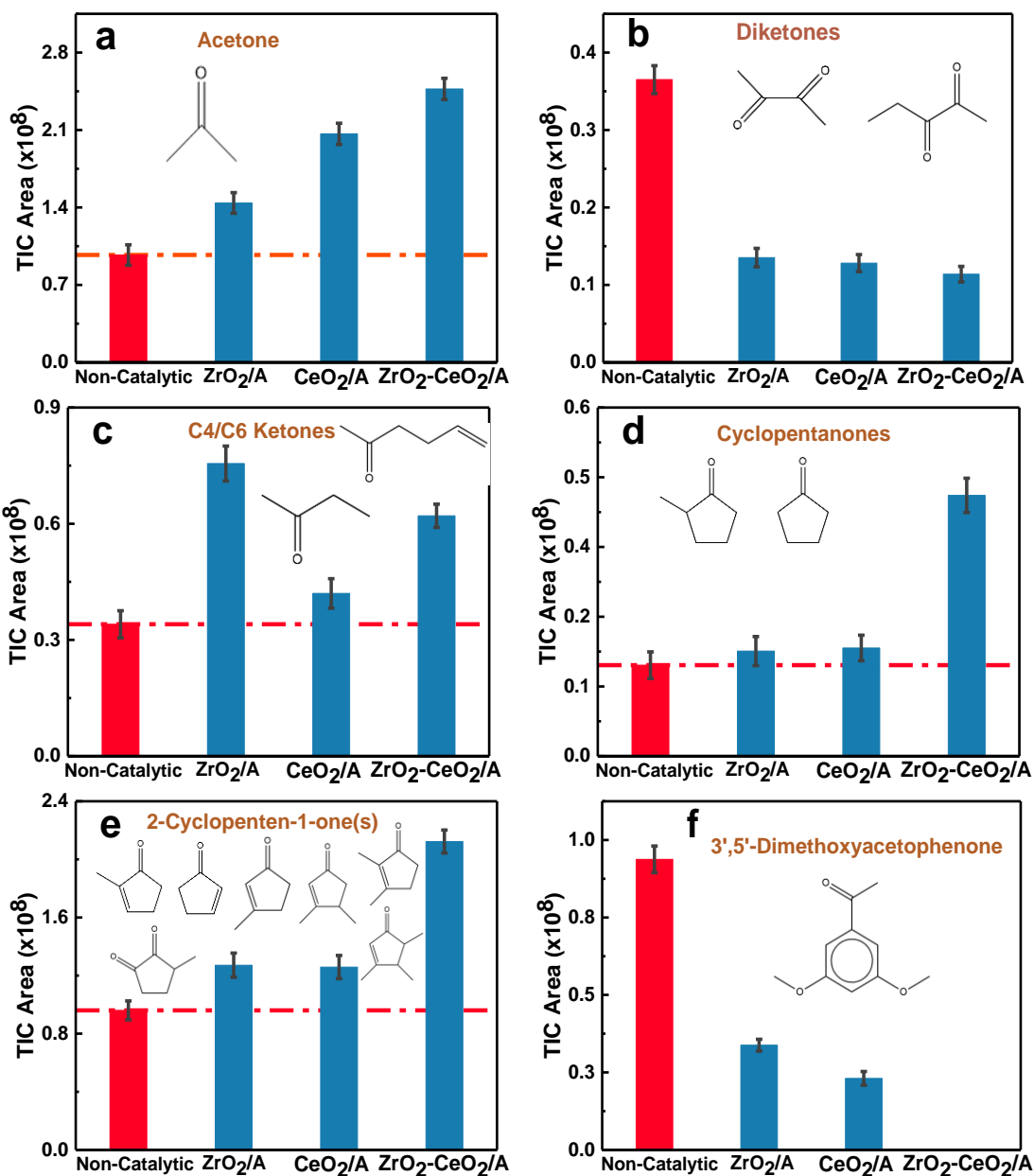
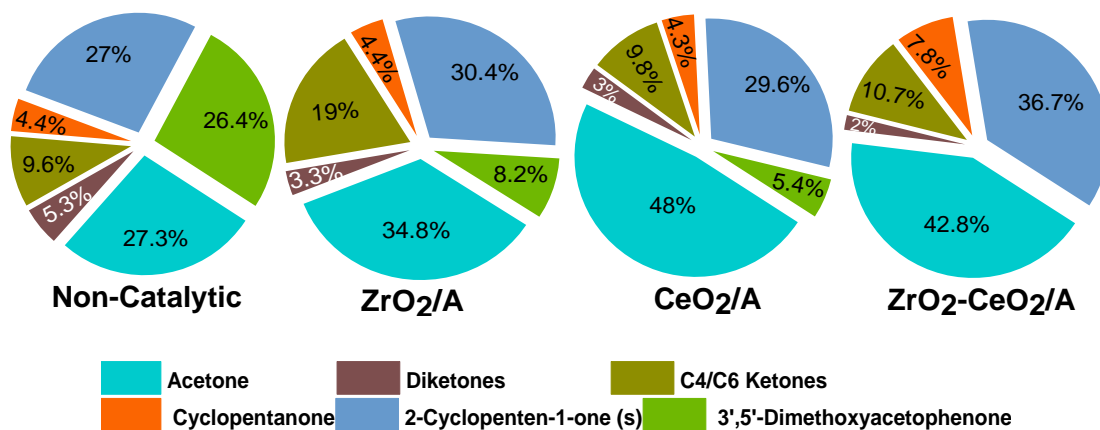


Figure 4. Distribution of ketones: (a) acetone; (b) diketones; (c) c4/c6 ketones; (d) cyclopentanones; (e) 2-cyclopenten-1-one (s); (f) 3,5-dimethoxyacetophenone.

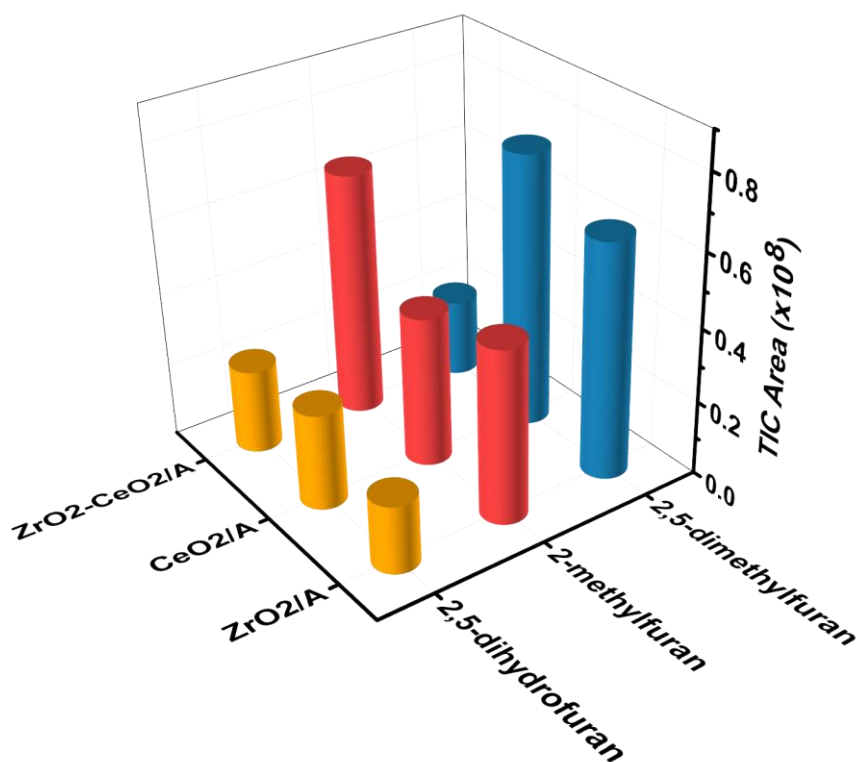


280

Figure 5. Relative selectivity of ketones.

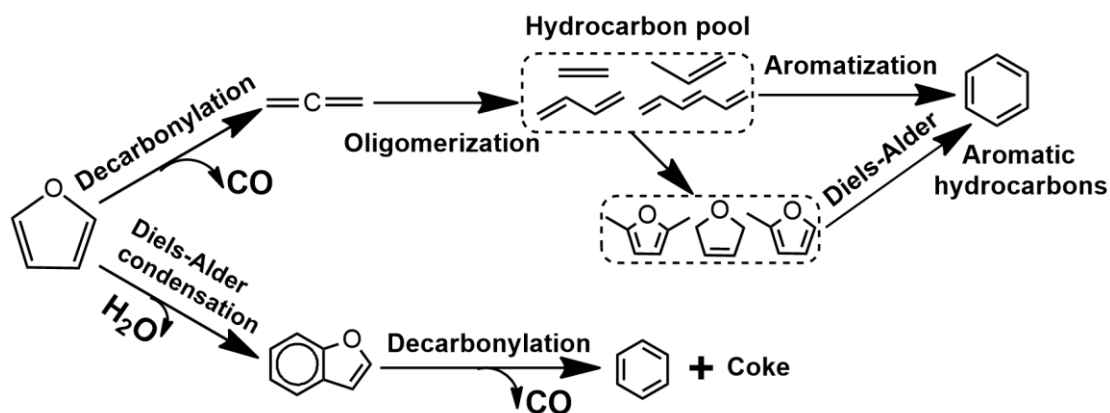
281 **Production of monofunctional furans**

282 Figure 6 presents the distribution of monofunctional furans. As shown, 2,5-
283 dimethylfuran was the most abundant compound in monofunctional furans and
284 followed by 2-methylfuran in CeO₂/γ-Al₂O₃ and ZrO₂/γ-Al₂O₃ catalyzed trials. Among
285 the metal oxides, CeO₂/γ-Al₂O₃ was more effective in the formation of 2,5-
286 dimethylfuran and 2,5-dihydrofuran when compared to other catalysts, while ZrO₂-
287 CeO₂/γ-Al₂O₃ facilitated the production of 2-methylfuran to the most extent.
288 Monofunctional furans are indispensable intermediates for the production of targeted
289 aromatic hydrocarbons. Huber and Cheng⁴⁰⁻⁴¹ investigated the conversion of furan over
290 ZSM-5 zeolites, and it was observed that furan first undergoes either decarbonylation
291 to produce allene (C₃H₄) and CO or condensation to produce benzofuran(C₈H₆O) and
292 water. Both allene and benzofuran are beneficial to the conversion of furan into
293 aromatic hydrocarbons as shown in Scheme 2. For instance, a number of olefins (often
294 referred to as “hydrocarbon pool”⁴²) can be produced by allene via oligomerization,
295 which leads to the formation of aromatic hydrocarbons via aromatization over ZSM-5.
296 Furthermore, the generated olefins also can react with furans to produce aromatic
297 hydrocarbons via Diels–Alder reaction. Hence, an increased production of
298 monofunctional furans in catalytic fast pyrolysis of bamboo sawdust facilitated the
299 formation of aromatic hydrocarbons which will be discussed in Section 3.3.



300

301 **Figure 6.** Distribution of monofunctional furans obtained from catalytic fast pyrolysis
 302 of bamboo sawdust over metal oxides.



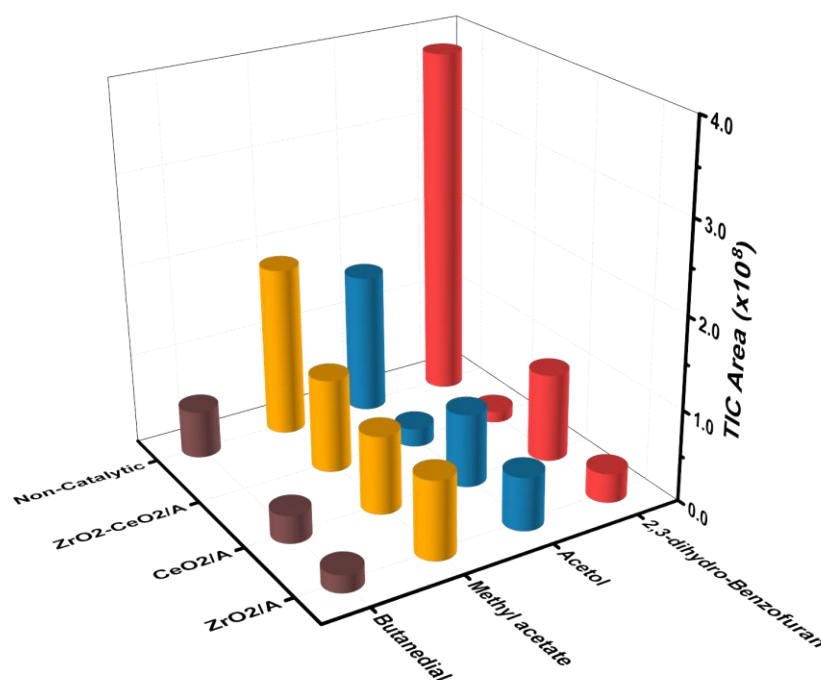
303

304 **Scheme 2.** Reaction pathway of converting furans into aromatic hydrocarbons using
 305 ZSM-5 zeolites ⁴⁰.

306 Conversion of other non-acidic pyrolytic oxygenates

307 As described above, converting other non-acidic pyrolytic oxygenates (such as acetol,
 308 methyl acetate, and butanedial) into ketones is an essential issue regarding the
 309 production of monofunctional hydrocarbon precursors. As shown in Figure 7, the use

310 of $\text{ZrO}_2\text{-CeO}_2/\gamma\text{-Al}_2\text{O}_3$ completely converted butanedial and performed a comparable
 311 catalytic activity with $\text{CeO}_2/\gamma\text{-Al}_2\text{O}_3$ in terms of the transformation of methyl acetate.
 312 Previous studies reported that aldehydes and esters could be converted to ketonic
 313 products through dimerization^{21, 43-44}. For instance, Gangadharan et al.⁴³ investigated
 314 the conversion of propanal over $\text{Ce}_x\text{Zr}_{1-x}\text{O}_2$ mixed metal oxides, and they found that
 315 propanal could be transformed to higher carbon chain oxygenates such as 3-pentanone
 316 and 3-heptanone via aldol condensation and ketonization. With respect to acetol, $\text{ZrO}_2\text{-}$
 317 $\text{CeO}_2/\gamma\text{-Al}_2\text{O}_3$ provided the highest conversion rate of 58.1% and followed by $\text{ZrO}_2/\gamma\text{-}$
 318 Al_2O_3 . Hakim et al.⁴⁵ investigated the conversion of acetol over CeZrO_x , and it was
 319 observed that C3–C6 carbonyls, such as acetone, 2-butanone, and 3-pentanone, were
 320 the main products, and the presence of acetol did not affect ketonization activity. In
 321 addition, Wan et al.⁴⁶ found that acetol could also be transformed to furans through
 322 cyclization, which was reflected in Figure 3f. Moreover, the formation of 2,3-
 323 dihydrobenzofuran was significantly suppressed when metal oxides were used to
 324 catalytic conversion of bamboo sawdust, and $\text{ZrO}_2\text{-CeO}_2/\gamma\text{-Al}_2\text{O}_3$ exhibited the most
 325 effective catalytic performance as a 95.5% conversion of 2,3-dihydrobenzofuran was
 326 obtained.



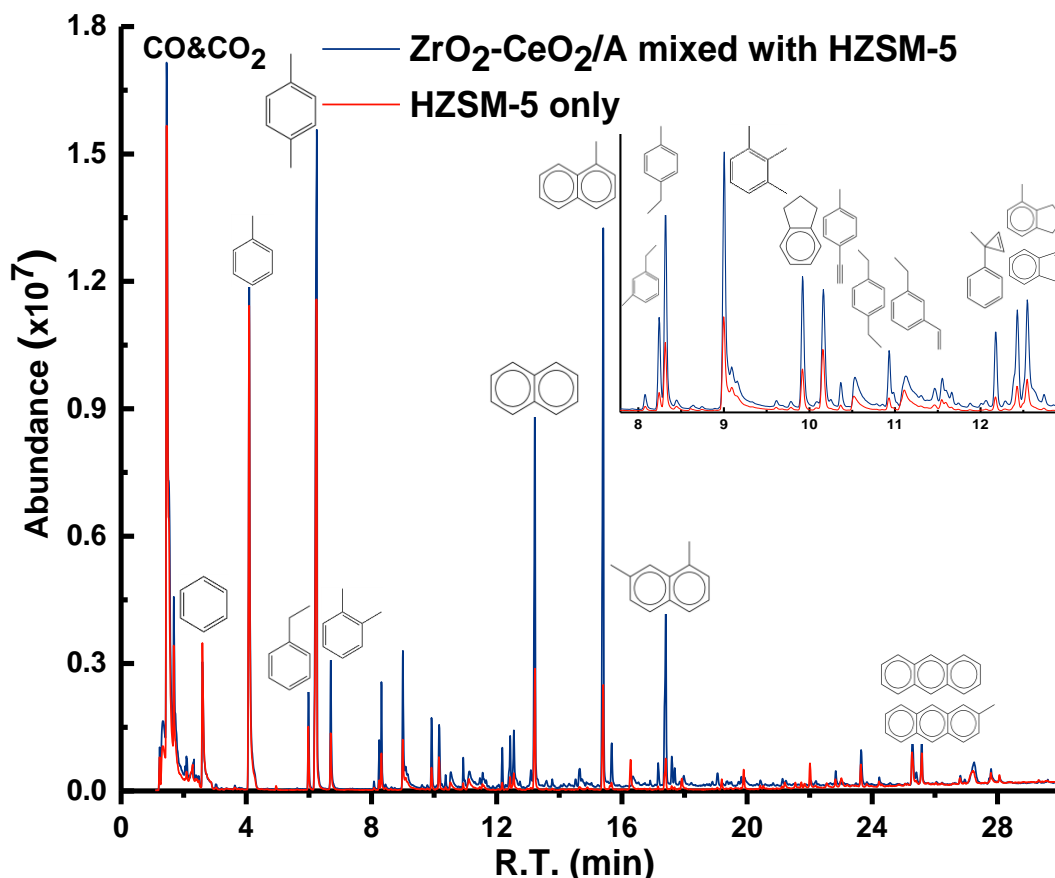
327

328 **Figure 7.** Catalytic conversion of non-acidic oxygenates over various metal oxides.

329 **Effect of a dual catalytic bed system on the formation of aromatic hydrocarbons**

330 As mentioned above, metal oxides promoted the formation of ketones and furans.
331 However, hydrocarbons are final desirable chemicals to be acquired from catalytic
332 reforming of pyrolysis oil. In this sense, acidic zeolites like HZSM-5 are more effective
333 in the production of aromatic hydrocarbons from catalytic conversion of biomass due
334 to its Brønsted acid sites and shape selectivity⁴⁷. Nevertheless, the microporous essence
335 of HZSM-5 limits diffusion of large oxygenated volatiles, and thus results in the
336 formation of coke which deactivates zeolites⁴⁸⁻⁴⁹. In present study, we use HZSM-5
337 and ZrO₂-CeO₂/γ-Al₂O₃ to form a dual catalytic bed system where the primary pyrolytic
338 products first encounter mesoporous ZrO₂-CeO₂/γ-Al₂O₃ to selective C-O cleavage and
339 C-C bonding and subsequently are catalyzed over HZSM-5 to form aromatic
340 hydrocarbons. Three different reaction combination pathways were investigated as
341 shown in Figure 1.

342 Figure 8 shows GC/MS chromatograms of primary pyrolytic products using ZrO₂-
343 CeO₂/γ-Al₂O₃ mixed with HZSM-5 (Mode II) and pure HZSM-5 catalytic pyrolysis
344 mode. As shown, the dominated compounds besides CO and CO₂ were monoaromatic
345 hydrocarbons and polyaromatic hydrocarbons (such as naphthalene and its derivatives).
346 Compared to pure HZSM-5 catalytic pyrolysis trial, the use of ZrO₂-CeO₂/γ-Al₂O₃
347 mixed with HZSM-5 mode significantly increased the production of aromatic
348 hydrocarbons. Furthermore, ketonic products were prominently converted, and a
349 complete conversion of furans was also observed, which indicated that hydrocarbon
350 precursors could be effectively converted into aromatic hydrocarbons when the dual
351 catalytic bed system was employed.



352

353 **Figure 8.** GC/MS chromatograms using $\text{ZrO}_2\text{-CeO}_2/\gamma\text{-Al}_2\text{O}_3$ mixed with HZSM-5
 354 mode and pure HZSM-5 during catalytic fast pyrolysis of bamboo sawdust.

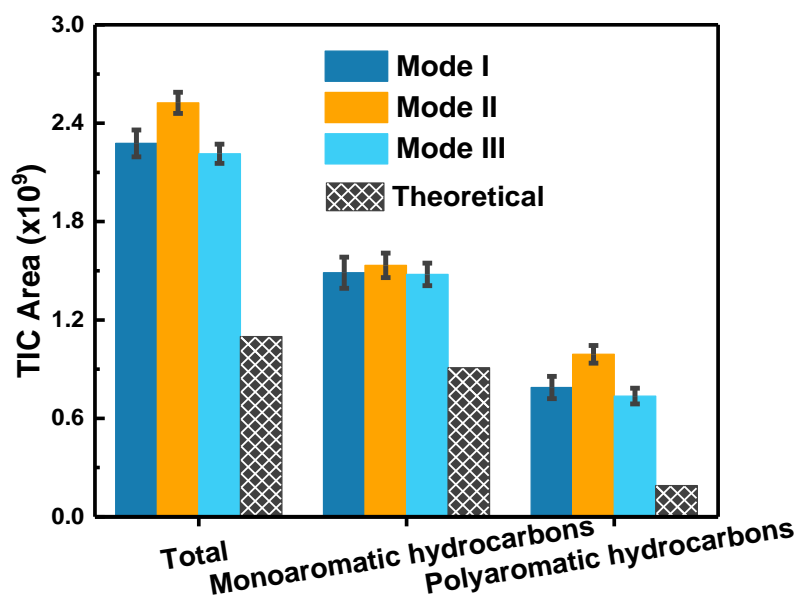
355 Figure 9 presents the aromatic hydrocarbons produced by catalytic fast pyrolysis of
 356 bamboo sawdust using various catalytic modes (detailed distributions shown in Table
 357 S9). The theoretical concentration was calculated by linear superposition of individual
 358 catalyst with the assumption of no interactions, which was shown as follows:

$$359 \quad \textit{Theoretical} = \frac{x_1 Y_{\text{HZSM-5}} + x_2 Y_{\text{oxides}}}{x_1 + x_2}$$

360 Where $Y_{\text{HZSM-5}}$ and Y_{oxides} are peak areas of specific products obtained from catalytic
 361 fast pyrolysis of bamboo sawdust over HZSM-5 only and metal oxides only,
 362 respectively. X_1 and X_2 are mass percentages of HZSM-5 and metal oxides in the total
 363 employed catalysts, respectively.

364 As indicated in Figure 9, all catalytic modes increased the concentration of aromatic
 365 hydrocarbons compared to theoretical one, which showed great promise for the
 366 upgrading of pyrolytic vapors. During the catalytic fast pyrolysis of bamboo sawdust

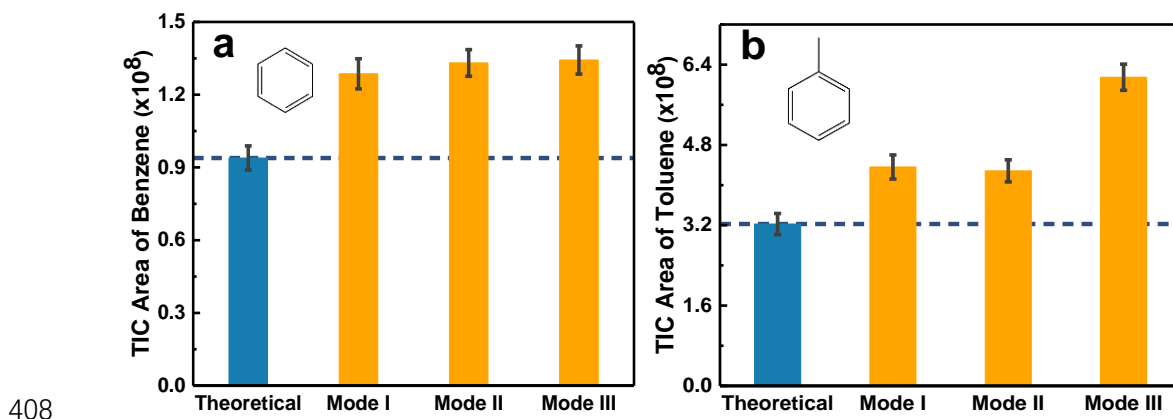
367 over combined metal oxide and HZSM-5, pyrolytic oxygenated compounds with large
 368 molecular weight were first fragmented into lower molecular weight hydrocarbon
 369 precursors by $\text{ZrO}_2\text{-CeO}_2/\gamma\text{-Al}_2\text{O}_3$, and subsequently were catalyzed over HZSM-5 to
 370 form aromatic hydrocarbons. Besides, mesoporous property of $\text{ZrO}_2\text{-CeO}_2/\gamma\text{-Al}_2\text{O}_3$ also
 371 favored the diffusion of pyrolytic vapors, resulting in enhanced mass transfer during
 372 the catalytic upgrading process. In particular, $\text{ZrO}_2\text{-CeO}_2/\gamma\text{-Al}_2\text{O}_3$ mixed with HZSM-
 373 5 catalytic pyrolysis run maximized the formation of aromatic hydrocarbons, and this
 374 might be attributed to the synergistic effect of $\text{ZrO}_2\text{-CeO}_2/\gamma\text{-Al}_2\text{O}_3$ and HZSM-5 which
 375 provides additional catalytic performance when the mixed mode was used. Moreover,
 376 for $\text{ZrO}_2\text{-CeO}_2/\gamma\text{-Al}_2\text{O}_3$ mixed with bamboo sawdust run (Mode III), the less increased
 377 formation of total aromatic hydrocarbons might be ascribed to insufficient contact of
 378 pyrolytic vapors and metal oxides which lowered the catalytic performance of $\text{ZrO}_2\text{-}$
 379 $\text{CeO}_2/\gamma\text{-Al}_2\text{O}_3$. However, the formation of polyaromatic hydrocarbons (PAHs) was
 380 difficult to avoid during the pyrolysis of biomass over HZSM-5 because of the
 381 hydrogen-deficient feature (i.e. low H/C effective ratio, 0~0.3) of biomass.

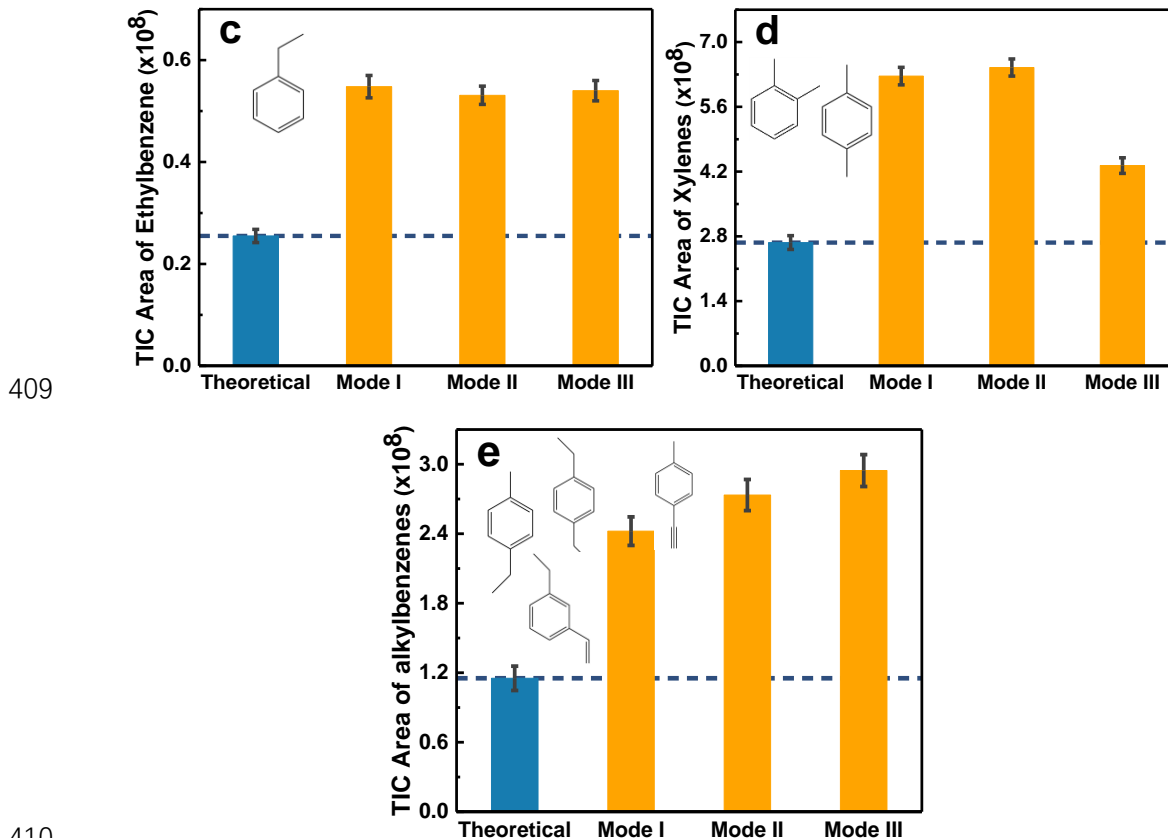


382
 383 **Figure 9.** Production of aromatic hydrocarbons as a function of various catalytic
 384 methods: Mode I: sequential $\text{ZrO}_2\text{-CeO}_2/\gamma\text{-Al}_2\text{O}_3$ and HZSM-5; Mode II: $\text{ZrO}_2\text{-}$
 385 $\text{CeO}_2/\gamma\text{-Al}_2\text{O}_3$ mixed with HZSM-5; Mode III: $\text{ZrO}_2\text{-CeO}_2/\gamma\text{-Al}_2\text{O}_3$ mixed with
 386 bamboo sawdust.

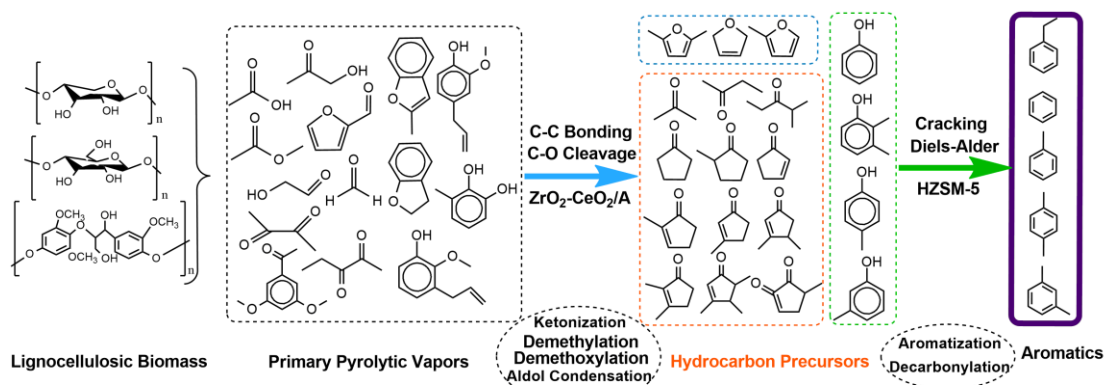
387 Figure 10 exhibits the distribution of monoaromatic hydrocarbons, such as benzene,

388 ethylbenzene, toluene, p-xylene, o-xylene, and alkylbenzenes. As shown, different
389 catalytic modes significantly affected the distribution of monoaromatic hydrocarbons
390 with toluene and xylenes being the dominated products. The $ZrO_2-CeO_2/\gamma-Al_2O_3$ mixed
391 with HZSM-5 (Mode II) and $ZrO_2-CeO_2/\gamma-Al_2O_3$ mixed with bamboo sawdust (Mode
392 III) trials produced a comparable concentration of benzene, while a slight decrease of
393 benzene was observed in sequential $ZrO_2-CeO_2/\gamma-Al_2O_3$ and HZSM-5 (Mode I). ZrO_2-
394 $CeO_2/\gamma-Al_2O_3$ mixed with bamboo sawdust catalytic pyrolysis run significantly
395 promoted the formation of toluene as a nearly 2-fold increase was obtained compared
396 to theoretical one. Moreover, all catalytic modes presented a comparable catalytic
397 performance in the production of ethylbenzene. With respect to alkylbenzenes, such as
398 1-ethyl-3-methylbenzene and 1-ethyl-4-methylbenzene, the concentration was
399 promoted in the order Mode III > Mode II > Mode I. Given the fact that the increase of
400 aromatic hydrocarbons was accompanied by decreased concentrations of ketones,
401 furans and other light oxygenates, a proposed mechanism was summarized in Figure
402 11⁸. As shown, oxygenated primary pyrolytic vapors first undergo selective C-O
403 cleavage and C-C bonding over $ZrO_2-CeO_2/\gamma-Al_2O_3$ to produce hydrocarbon fuel
404 precursors (including monofunctional furans, linear and cyclic ketones, and
405 alkylphenols) via ketonization, aldol condensation, demethylation and demethoxylation,
406 and then the hydrocarbon fuel precursors are catalyzed by HZSM-5 to form aromatic
407 hydrocarbons.





411 **Figure 10.** Distribution of monoaromatic hydrocarbons obtained from catalytic fast
 412 pyrolysis of bamboo sawdust using different catalytic modes: (a) benzene; (b)
 413 toluene; (c) ethylbenzene; (d) xylenes; (e) alkylbenzenes.



415 **Figure 11.** Proposed reaction pathways for the production of aromatic hydrocarbons
 416 using a dual catalytic bed system.

417 **Conclusions**

418 In summary, catalytic fast pyrolysis of bamboo sawdust over synthesized ZrO_2/γ -

419 Al₂O₃, CeO₂/γ-Al₂O₃, and ZrO₂-CeO₂/γ-Al₂O₃ promoted the formation of ketonic
420 products, and the highest concentration of ketones could be achieved over ZrO₂-
421 CeO₂/γ-Al₂O₃, along with the lowest formation of acids. Linear and cyclic ketones were
422 dominant components in ketonic products, and the use of ZrO₂-CeO₂/γ-Al₂O₃ increased
423 the relative selectivity of cyclic ketones from 31.5% (noncatalytic pyrolysis run) to
424 44.2%. A complete elimination of 3,5-dimethoxyacetophenone also was obtained using
425 ZrO₂-CeO₂/γ-Al₂O₃. In addition, furfural was fully converted into monofunctional
426 furans when metal oxides were used, and the maximum concentration of 2,5-
427 dimethylfuran and 2-methylfuran could be obtained over CeO₂/γ-Al₂O₃ and ZrO₂-
428 CeO₂/γ-Al₂O₃, respectively. Non-acidic oxygenates were also investigated in terms of
429 the formation of ketones, and acetol, methyl acetate, as well as butanedial could be
430 effectively converted into ketones over ZrO₂-CeO₂/γ-Al₂O₃. The dual catalytic bed
431 system facilitated the production of aromatic hydrocarbons, and ZrO₂-CeO₂/γ-Al₂O₃
432 mixed with HZSM-5 catalytic mode increased the concentration of aromatic
433 hydrocarbons to the greatest extent. In contrast, ZrO₂-CeO₂/γ-Al₂O₃ mixed with
434 bamboo sawdust mode produced more toluene and alkylbenzenes.

435 **ASSOCIATED CONTENT**

436 **Supporting Information**

437 The supporting information is available on the ACS website.

438 Physicochemical properties of HZSM-5. Picture of Py-GC/MS. Nitrogen
439 adsorption–desorption isotherms and NH₃-TPD results of synthesized metal oxides.
440 Detailed pyrolytic products obtained from fast pyrolysis of bamboo sawdust
441 with/without catalysts. Major products derived from catalytic fast pyrolysis of bamboo
442 sawdust over ZrO₂-CeO₂/γ-Al₂O₃ at different catalyst/biomass mass ratios ranging from
443 4:1 to 8:1. Detailed distributions of aromatic hydrocarbons using various modes.

444 **Author Information**

445 **Corresponding authors:**

446 *Phone/fax: +86 25 83794700; E-mail address: zzhong@seu.edu.cn;

447 *Fax: 865-974-7076; Tel: 865-974-2042; E-mail: aragausk@utk.edu.

448 **ORCID**

449 Xianzhi Meng: 0000-0003-4303-3403

450 Arthur J. Ragauskas: 0000-0002-3536-554X

451 **Author Contributions**

452 ※ These authors contributed equally to this work.

453 **Notes**

454 The authors declare no competing financial interest.

455 **Acknowledgments**

456 The authors are grateful for the National Natural Science Fund Program of China
457 (No. 51776042), the Scientific Research Foundation of Graduate School of Southeast
458 University (YBJJ1646), the Scientific Innovation Research Program of College
459 Graduate in Jiangsu Province (KYLX16_0204) as well as the Financial Support from
460 the Program of China Scholarships Council (No. 201706090032).

461 **References**

- 462 1. Ragauskas, A. J.; Beckham, G. T.; Biddy, M. J.; Chandra, R.; Chen, F.; Davis, M.
463 F.; Davison, B. H.; Dixon, R. A.; Gilna, P.; Keller, M.; Langan, P.; Naskar, A. K.;
464 Saddler, J. N.; Tschaplinski, T. J.; Tuskan, G. A.; Wyman, C. E., Lignin valorization:
465 improving lignin processing in the biorefinery. *Science* **2014**, *344* (6185), 1246843.
- 466 2. Ben, H.; Huang, F.; Li, L.; Ragauskas, A. J., In situ upgrading of whole biomass to
467 biofuel precursors with low average molecular weight and acidity by the use of zeolite
468 mixture. *RSC Adv.* **2015**, *5* (91), 74821-74827.

- 469 3. Yunpu, W.; Leilei, D. A. I.; Liangliang, F. A. N.; Shaoqi, S.; Yuhuan, L. I. U.; Roger,
470 R., Review of microwave-assisted lignin conversion for renewable fuels and chemicals.
471 *J. Anal. Appl. Pyrolysis* **2016**, *119*, 104-113.
- 472 4. Borges, F. C.; Xie, Q.; Min, M.; Muniz, L. A.; Farenzena, M.; Trierweiler, J. O.;
473 Chen, P.; Ruan, R., Fast microwave-assisted pyrolysis of microalgae using microwave
474 absorbent and HZSM-5 catalyst. *Bioresour. Technol.* **2014**, *166*, 518-26.
- 475 5. Iisa, K.; French, R. J.; Orton, K. A.; Dutta, A.; Schaidle, J. A., Production of low-
476 oxygen bio-oil via ex situ catalytic fast pyrolysis and hydrotreating. *Fuel* **2017**, *207*,
477 413-422.
- 478 6. Hao, N.; Bezerra, T. L.; Wu, Q.; Ben, H.; Sun, Q.; Adhikari, S.; Ragauskas, A. J.,
479 Effect of autohydrolysis pretreatment on biomass structure and the resulting bio-oil
480 from a pyrolysis process. *Fuel* **2017**, *206*, 494-503.
- 481 7. Mullen, C. A.; Tarves, P. C.; Boateng, A. A., Role of Potassium Exchange in
482 Catalytic Pyrolysis of Biomass over ZSM-5: Formation of Alkyl Phenols and Furans.
483 *ACS Sustainable Chem. Eng.* **2017**, *5* (3), 2154-2162.
- 484 8. Mante, O. D.; Rodriguez, J. A.; Senanayake, S. D.; Babu, S. P., Catalytic
485 conversion of biomass pyrolysis vapors into hydrocarbon fuel precursors. *Green Chem.*
486 **2015**, *17* (4), 2362-2368.
- 487 9. Gao, H.; Liu, H.; Pang, B.; Yu, G.; Du, J.; Zhang, Y.; Wang, H.; Mu, X., Production
488 of furfural from waste aqueous hemicellulose solution of hardwood over ZSM-5 zeolite.
489 *Bioresour. Technol.* **2014**, *172*, 453-456.
- 490 10. Iisa, K.; Robichaud, D. J.; Watson, M. J.; ten Dam, J.; Dutta, A.; Mukarakate, C.;
491 Kim, S.; Nimlos, M. R.; Baldwin, R. M., Improving biomass pyrolysis economics by
492 integrating vapor and liquid phase upgrading. *Green Chem.* **2018**, *20* (3), 567-582.
- 493 11. Cao, Z.; Engelhardt, J.; Dierks, M.; Clough, M. T.; Wang, G. H.; Heracleous, E.;
494 Lappas, A.; Rinaldi, R.; Schuth, F., Catalysis Meets Nonthermal Separation for the
495 Production of (Alkyl)phenols and Hydrocarbons from Pyrolysis Oil. *Angew. Chem.*
496 **2017**, *56* (9), 2334-2339.
- 497 12. Mettler, M. S.; Mushrif, S. H.; Paulsen, A. D.; Javadekar, A. D.; Vlachos, D. G.;
498 Dauenhauer, P. J., Revealing pyrolysis chemistry for biofuels production: Conversion

499 of cellulose to furans and small oxygenates. *Energy Environ. Sci.* **2012**, *5* (1), 5414-
500 5424.

501 13. Bohre, A.; Saha, B.; Abu-Omar, M. M., Catalytic Upgrading of 5-
502 Hydroxymethylfurfural to Drop-in Biofuels by Solid Base and Bifunctional Metal-Acid
503 Catalysts. *ChemSusChem* **2015**, *8* (23), 4022-9.

504 14. Sacia, E. R.; Balakrishnan, M.; Deaner, M. H.; Goulas, K. A.; Toste, F. D.; Bell, A.
505 T., Highly selective condensation of biomass-derived methyl ketones as a source of
506 aviation fuel. *ChemSusChem* **2015**, *8* (10), 1726-36.

507 15. Zhang, Y.; Cui, H.; Yi, W.; Song, F.; Zhao, P.; Wang, L.; Cui, J., Highly effective
508 decarboxylation of the carboxylic acids in fast pyrolysis oil of rice husk towards ketones
509 using CaCO₃ as a recyclable agent. *Biomass and Bioenergy* **2017**, *102*, 13-22.

510 16. Pham, T. N.; Shi, D.; Sooknoi, T.; Resasco, D. E., Aqueous-phase ketonization of
511 acetic acid over Ru/TiO₂/carbon catalysts. *J. Catal.* **2012**, *295*, 169-178.

512 17. Wu, K.; Yang, M.; Pu, W.; Wu, Y.; Shi, Y.; Hu, H.-s., Carbon Promoted ZrO₂
513 Catalysts for Aqueous-Phase Ketonization of Acetic Acid. *ACS Sustainable Chem. Eng.*
514 **2017**, *5* (4), 3509-3516.

515 18. Pacchioni, G., Ketonization of Carboxylic Acids in Biomass Conversion over TiO₂
516 and ZrO₂ Surfaces: A DFT Perspective. *ACS Catal.* **2014**, *4* (9), 2874-2888.

517 19. Lu, F.; Jiang, B.; Wang, J.; Huang, Z.; Liao, Z.; Yang, Y.; Zheng, J., Promotional
518 effect of Ti doping on the ketonization of acetic acid over a CeO₂ catalyst. *RSC Adv.*
519 **2017**, *7* (36), 22017-22026.

520 20. Mekhemer, G.; Halawy, S.; Mohamed, M.; Zaki, M., Ketonization of acetic acid
521 vapour over polycrystalline magnesia: in situ Fourier transform infrared spectroscopy
522 and kinetic studies. *J. Catal.* **2005**, *230* (1), 109-122.

523 21. Nagashima, O.; Sato, S.; Takahashi, R.; Sodesawa, T., Ketonization of carboxylic
524 acids over CeO₂-based composite oxides. *J. Mol. Catal. A: Chem.: Chemical* **2005**, *227*
525 (1-2), 231-239.

526 22. Pham, T. N.; Sooknoi, T.; Crossley, S. P.; Resasco, D. E., Ketonization of
527 Carboxylic Acids: Mechanisms, Catalysts, and Implications for Biomass Conversion.
528 *ACS Catal.* **2013**, *3* (11), 2456-2473.

- 529 23. Oasmaa, A.; Elliott, D. C.; Korhonen, J., Acidity of Biomass Fast Pyrolysis Bio-
530 oils. *Energy Fuels* **2010**, *24* (12), 6548-6554.
- 531 24. Tang, C.; Li, J.; Yao, X.; Sun, J.; Cao, Y.; Zhang, L.; Gao, F.; Deng, Y.; Dong, L.,
532 Mesoporous NiO–CeO₂ catalysts for CO oxidation: Nickel content effect and
533 mechanism aspect. *Appl. Catal., A* **2015**, *494*, 77-86.
- 534 25. Krishna, K.; Bueno-López, A.; Makkee, M.; Moulijn, J. A., Potential rare earth
535 modified CeO₂ catalysts for soot oxidation. *Appl. Catal., B* **2007**, *75* (3-4), 189-200.
- 536 26. Wang, W.; Wu, K.; Liu, P.; Li, L.; Yang, Y.; Wang, Y., Hydrodeoxygenation of p-
537 Cresol over Pt/Al₂O₃ Catalyst Promoted by ZrO₂, CeO₂, and CeO₂–ZrO₂. *Ind. Eng.*
538 *Chem. Res.* **2016**, *55* (28), 7598-7603.
- 539 27. Zhang, M.; Resende, F. L. P.; Moutsoglou, A., Catalytic fast pyrolysis of aspen
540 lignin via Py-GC/MS. *Fuel* **2014**, *116*, 358-369.
- 541 28. Wang, J.; Zhang, B.; Zhong, Z.; Ding, K.; Deng, A.; Min, M.; Chen, P.; Ruan, R.,
542 Catalytic fast co-pyrolysis of bamboo residual and waste lubricating oil over an ex-situ
543 dual catalytic beds of MgO and HZSM-5: Analytical PY-GC/MS study. *Energy Convers.*
544 *Manage.* **2017**, *139*, 222-231.
- 545 29. Wang, J.; Zhong, Z.; Ding, K.; Zhang, B.; Deng, A.; Min, M.; Chen, P.; Ruan, R.,
546 Co-pyrolysis of bamboo residual with waste tire over dual catalytic stage of CaO and
547 co-modified HZSM-5. *Energy* **2017**, *133*, 90-98.
- 548 30. Lu, Q.; Zhou, M.-x.; Li, W.-t.; Wang, X.; Cui, M.-s.; Yang, Y.-p., Catalytic fast
549 pyrolysis of biomass with noble metal-like catalysts to produce high-grade bio-oil:
550 Analytical Py-GC/MS study. *Catal. Today* **2018**, *302*, 169-179.
- 551 31. Sebestyén, Z.; Barta-Rajnai, E.; Bozi, J.; Blazsó, M.; Jakab, E.; Miskolczi, N.; Sója,
552 J.; Czégény, Z., Thermo-catalytic pyrolysis of biomass and plastic mixtures using
553 HZSM-5. *Appl. Energy* **2017**, *207*, 114-122.
- 554 32. Putrakumar, B.; Nagaraju, N.; Kumar, V. P.; Chary, K. V. R., Hydrogenation of
555 levulinic acid to γ -valerolactone over copper catalysts supported on γ -Al₂O₃. *Catal.*
556 *Today* **2015**, *250*, 209-217.
- 557 33. Stefanidis, S. D.; Karakoulia, S. A.; Kalogiannis, K. G.; Iliopoulou, E. F.; Delimitis,
558 A.; Yiannoulakis, H.; Zampetakis, T.; Lappas, A. A.; Triantafyllidis, K. S., Natural

- 559 magnesium oxide (MgO) catalysts: A cost-effective sustainable alternative to acid
560 zeolites for the in situ upgrading of biomass fast pyrolysis oil. *Appl. Catal., B* **2016**,
561 *196*, 155-173.
- 562 34. Kumar, R.; Enjamuri, N.; Shah, S.; Al-Fatesh, A. S.; Bravo-Suárez, J. J.;
563 Chowdhury, B., Ketonization of oxygenated hydrocarbons on metal oxide based
564 catalysts. *Catal. Today* **2018**, *302*, 16-49.
- 565 35. Wang, J.; Zhong, Z.; Ding, K.; Xue, Z., Catalytic fast pyrolysis of mushroom waste
566 to upgraded bio-oil products via pre-coked modified HZSM-5 catalyst. *Bioresour.*
567 *Technol.* **2016**, *212*, 6-10.
- 568 36. Snell, R. W.; Shanks, B. H., Insights into the Ceria-Catalyzed Ketonization
569 Reaction for Biofuels Applications. *ACS Catal.* **2013**, *3* (4), 783-789.
- 570 37. Grams, J.; Niewiadomski, M.; Ruppert, A. M.; Kwapiński, W., Catalytic
571 performance of a Ni catalyst supported on CeO₂, ZrO₂ and CeO₂-ZrO₂ in the upgrading
572 of cellulose fast pyrolysis vapors. *C.R. Chim.* **2015**, *18* (11), 1223-1228.
- 573 38. Lou, R.; Wu, S.-b.; Lv, G.-j., Effect of conditions on fast pyrolysis of bamboo lignin.
574 *J. Anal. Appl. Pyrolysis* **2010**, *89* (2), 191-196.
- 575 39. Dong, Q.; Zhang, S.; Zhang, L.; Ding, K.; Xiong, Y., Effects of four types of dilute
576 acid washing on moso bamboo pyrolysis using Py-GC/MS. *Bioresour. Technol.* **2015**,
577 *185*, 62-69.
- 578 40. Cheng, Y. T.; Jae, J.; Shi, J.; Fan, W.; Huber, G. W., Production of renewable
579 aromatic compounds by catalytic fast pyrolysis of lignocellulosic biomass with
580 bifunctional Ga/ZSM-5 catalysts. *Angew. Chem.* **2012**, *51* (6), 1387-1390.
- 581 41. Gou, J.; Wang, Z.; Li, C.; Qi, X.; Vattipalli, V.; Cheng, Y.-T.; Huber, G.; Conner,
582 W. C.; Dauenhauer, P. J.; Mountziaris, T. J.; Fan, W., The effects of ZSM-5
583 mesoporosity and morphology on the catalytic fast pyrolysis of furan. *Green Chem.*
584 **2017**, *19* (15), 3549-3557.
- 585 42. Cheng, Y.-T.; Huber, G. W., Production of targeted aromatics by using Diels-Alder
586 classes of reactions with furans and olefins over ZSM-5. *Green Chem.* **2012**, *14* (11),
587 3114-3125.
- 588 43. Gangadharan, A.; Shen, M.; Sooknoi, T.; Resasco, D. E.; Mallinson, R. G.,

589 Condensation reactions of propanal over $Ce_xZr_{1-x}O_2$ mixed oxide catalysts. *Appl. Catal.,*
590 *A* **2010**, 385 (1-2), 80-91.

591 44. Kamimura, Y.; Sato, S.; Takahashi, R.; Sodesawa, T.; Akashi, T., Synthesis of 3-
592 pentanone from 1-propanol over $CeO_2-Fe_2O_3$ catalysts. *Appl. Catal., A* **2003**, 252 (2),
593 399-410.

594 45. Hakim, S. H.; Shanks, B. H.; Dumesic, J. A., Catalytic upgrading of the light
595 fraction of a simulated bio-oil over CeZrOx catalyst. *Appl. Catal., B* **2013**, 142-143,
596 368-376.

597 46. Wan, S.; Pham, T.; Zhang, S.; Lobban, L.; Resasco, D.; Mallinson, R., Direct
598 catalytic upgrading of biomass pyrolysis vapors by a dual function Ru/TiO₂catalyst.
599 *AIChE J.* **2013**, 59 (7), 2275-2285.

600 47. Ben, H.; Ragauskas, A. J., Influence of Si/Al Ratio of ZSM-5 Zeolite on the
601 Properties of Lignin Pyrolysis Products. *ACS Sustainable Chem. Eng.* **2013**, 1 (3), 316-
602 324.

603 48. Kim, Y.-M.; Jae, J.; Kim, B.-S.; Hong, Y.; Jung, S.-C.; Park, Y.-K., Catalytic co-
604 pyrolysis of torrefied yellow poplar and high-density polyethylene using microporous
605 HZSM-5 and mesoporous Al-MCM-41 catalysts. *Energy Convers. Manage.* **2017**, 149,
606 966-973.

607 49. Shao, S.; Zhang, H.; Wang, Y.; Xiao, R.; Heng, L.; Shen, D., Catalytic Pyrolysis of
608 Biomass-Derived Compounds: Coking Kinetics and Formation Network. *Energy Fuels*
609 **2015**, 29 (3), 1751-1757.

610